GEORGIA INSTITUTE OF TECHNOLOGY — OFFICE OF CONTRACT ADMINISTRATION

PROJECT ADMINISTRATION DATA SHEET

[x] ORIGINAL [ ] REVISION NO. ____

Project No. A-3507 GTRI/~~GIT~~ DATE 4/4/83

Project Director: Wallace Shakun & John Brown ~~School~~/Lab EMSL

Sponsor: Westinghouse Electric Corporation

Type Agreement: P. O. No. 76-37262-S (modified)

Award Period: From 3/22/83 To ~~4/30/83~~ (Performance) 4/30/83 (Reports)

Sponsor Amount: Total Estimated: $ 6,056 Funded: $ 6,056

Cost Sharing Amount: $ Cost Sharing No:

Title: Transformer Insulation Failure

ADMINISTRATIVE DATA OCA Contact Frank Huff

1) Sponsor Technical Contact:

Westinghouse Electric Co.
Newton Bridge Road
Athens, Ga. 30613

Attn: L. W. Mesta

2) Sponsor Admin/Contractual Matters:

Westinghouse Electric Co.
Newton Bridge Rd.
Athens, Ga. 30613

Attn: Richard D. Buckley
Mgr. Materials Div.

Defense Priority Rating: NA

Military Security Classification:

(or) Company/Industrial Proprietary: See below

RESTRICTIONS

See Attached ____ Supplemental Information Sheet for Additional Requirements.

Travel: Foreign travel must have prior approval – Contact OCA in each case. Domestic travel requires sponsor approval where total will exceed greater of $500 or 125% of approved proposal budget category.

Equipment: Title vests with NA; none proposed

COMMENTS:

Budget includes $500 patent and data rights fee. Information developed or communicated to Georgia Tech in performance of this project is considered highly confidential and prior written approval for disclosure of such information is required.

COPIES TO:

Research Administrative Network
Research Property Management
Accounting
Procurement/EES Supply Services
Research Security Services
~~Reports Coordinator (OCA)~~
GTRI
Library
Research Communications (2)
Project File
Other Wallace, Shakun/Brown
Other

GEORGIA INSTITUTE OF TECHNOLOGY OFFICE OF CONTRACT ADMINISTRATION

SPONSORED PROJECT TERMINATION/CLOSEOUT SHEET

Date 10/28/83

Project No. A-3507 ~~School~~/Lab EMSL

Includes Subproject No.(s) _____

Project Director(s) Drs. Wallace Shakun & John Brown GTRI / ~~GIT~~

Sponsor Westinghouse Electric Corp.

Title Transformer Insulation Failure

Effective Completion Date: 11/30/83 (Performance) 11/30/83 (Reports)

Grant/Contract Closeout Actions Remaining:

- [ ] None
- [x] Final Invoice or Final Fiscal Report
- [ ] Closing Documents
- [x] Final Report of Inventions
- [ ] Govt. Property Inventory & Related Certificate
- [ ] Classified Material Certificate
- [ ] Other _____

Continues Project No. _____ Continued by Project No. _____

COPIES TO:

Project Director
Research Administrative Network
Research Property Management
Accounting
Procurement/EES Supply Services
Research Security Services
Reports Coordinator (OCA)
Legal Services

Library
GTRI
Research Communications (2)
Project File
Other _____

Form OCA 60-1028

Interim Summary Report

Transformer Insulation Failure

July 21, 1983

Prepared by

John L. Brown
Dr. Wallace Shakun

Prepared for

Westinghouse Electric Company
Newton Bridge Road
Athens, Georgia 30613

Submitted by

Energy and Materials Sciences Laboratory
Engineering Experiment Station
Georgia Institute of Technology
Atlanta, Georgia 30332

Contracting through

GEORGIA TECH RESEARCH INSTITUTE
Georgia Institute of Technology
Atlanta, Georgia 30332

Table of Contents

Abstract

This report summarizes the results of analyzing and concludes the probable cause for the "cracks" appearing on mill flattened and enamelled wire samples.

Conclusion

(1) SEM analysis of the samples indicate that the cracks are the result of strain relief within the formvar.

(2) The material properties of formvar appear to have insufficient plasticity to control crack formation.

(3) The sample material PDG 940 shows considerable cracking, the sample labeled 544-2 appears to have less cracking potential (more ductile).

Probable Variables Resulting in Cracking

(1) Temperature differences during curing

(2) Strain relieving, beyond yield zone

(3) Irregular substrate surface

(4) Contamination on the surface

(5) Poor bonding to the substrate

(6) Too sharp radius or curvature of the wire

(7) Viscosity too low for process flow rate

(8) Gas or water droplets trapped in formvar insulation.

(9) Inorganic impurities within the formvar material.

Data Review

1. The photographs taken (Figure 1, 2) under polarized light indicate that there are strain fields around the incipient cracks in the formvar. Striations are evident at right angles to the aluminum wire longitudinal axis.

2. There appears in the Cu wire evidence of incipient cracks (Figures 3, 4) similar to that which occurs in the aluminum wire.

3. Scanning electron microscopy (SEM) techniques were utilized with the following summary results:
   a. Copper wire (.102 - flattened) was dissolved in dilute HNO_3 to recover insulation. The convex side of the wire shows more light polarization contrast under PLM than the flat sides. Some parallel striations appear at right angles to the wire axis as seen by transmission light microscope (TLM). The striations may be indicative of strain relief effects taking place in the formvar.
   b. The aluminum wire was dissolved in dilute HCL and took longer than the Cu in HNO_3. Formvar insulation was recovered from a one inch portion of round (unflattened) and flattened wire;the flattened wire is darker in color than the round-unrolled when placed between a micro slide with glycerine. By TLM it was possible to observe cracks and strain relief patterns around the visible cracks as the acid etched into the formvar. Figure 5, 6 and 7 illustrate the characteristics of cracking in formvar on alumium wire. As the magnification increases the crack propogation path can be more readily seen (Figure 7, 520X).
   c. Scanning electron microscopy of the copper wire insulation (Figure 8,9) shows ductile fracture tendrils in the formvar. Ripples and smaller cracks appear near major regions of cracking of the formvar. The cracks under high magnification indicate tendrils which may be indicative of excessive local heating.
   d. Formvar varnish samples were tested for characteristics when dried on a

flat glass slide. Figures 10 and 11 illustrate on a first order basis that if the samples (PDG 940 and 544-2) are dried under high temperature (rapidly) brittle fracture results. When the samples were air dried (room temperature) or over a long period, the insulation materials appear to have more ductile features (Figures 12 and 13).

Areas for Investigation

(1) Determine the degree of cross linking in the polymers.

(2) Determine the feasibility of bond strength or pull strength between the insulation and the wire substrate.

Microscopic Photographs

OPTICAL - POLARIZED LIGHT

UNCROSSED POLARS

CROSSED POLARS

Crack in formvar on Al wire. Polarized light shows strain field around crack

FIGURE 1

OPTICAL - POLARIZED LIGHT

Striations at right angles to wire axis

These are incipient cracks in insulation on Al wire

FIGURE 2

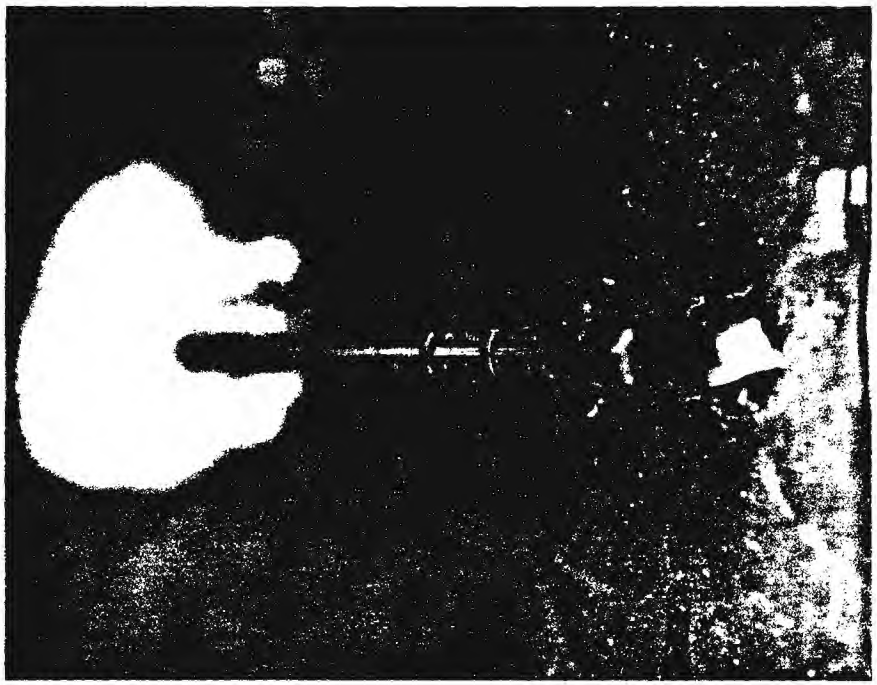

FIGURE 3

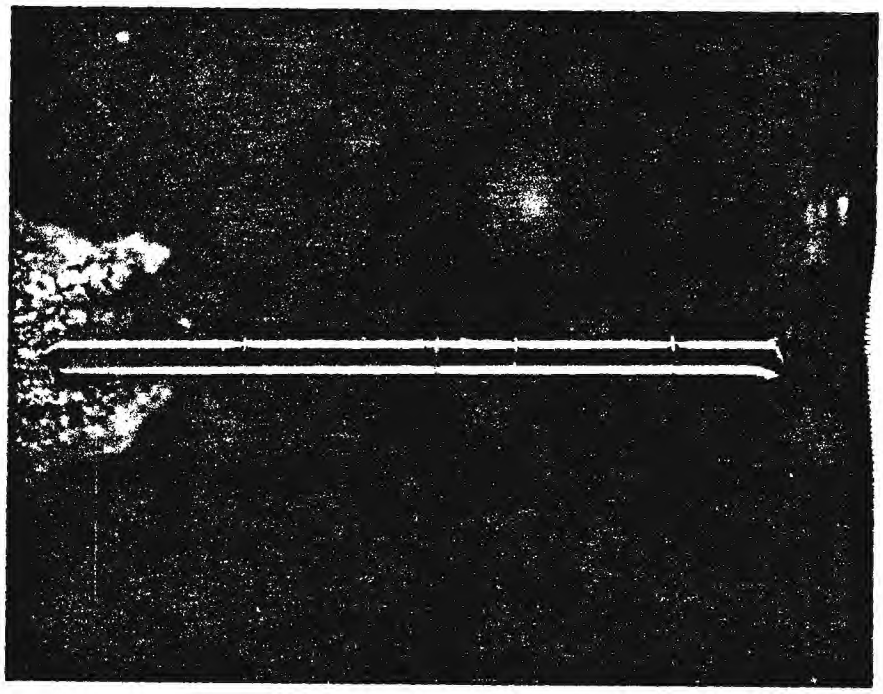

FIGURE 4

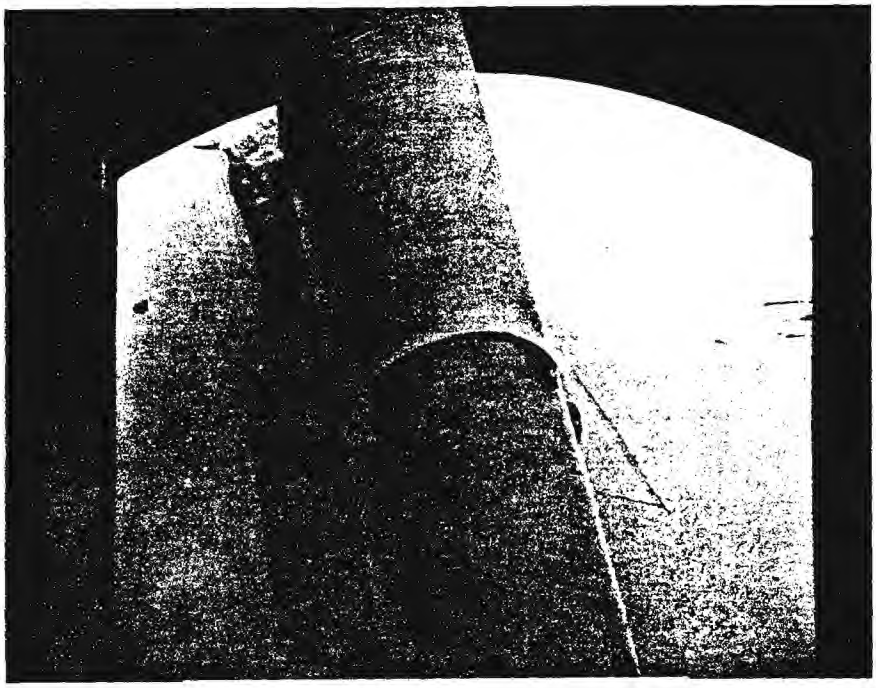

A1 96X

FIGURE 5

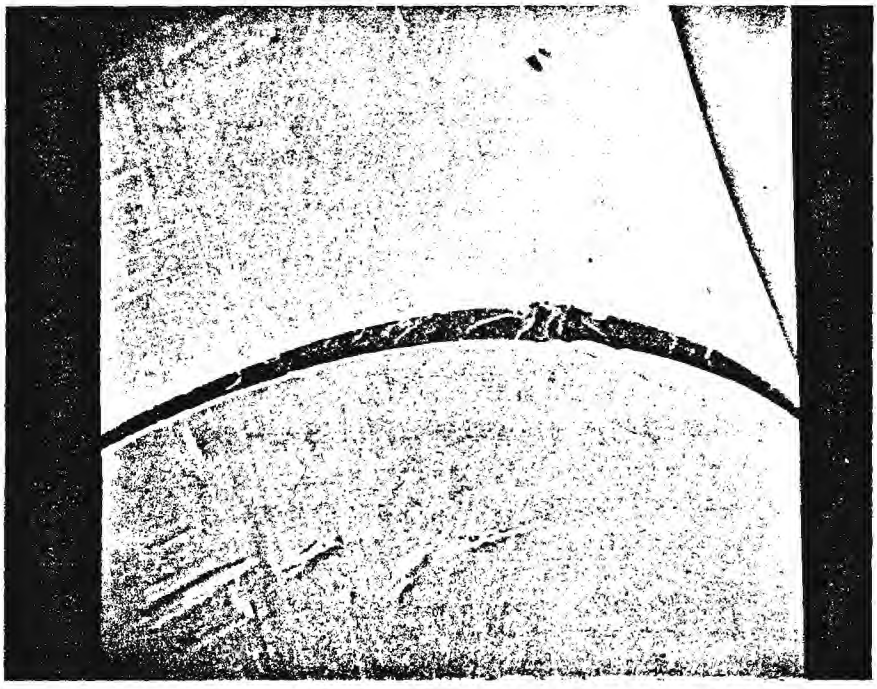

A1 22X

FIGURE 6

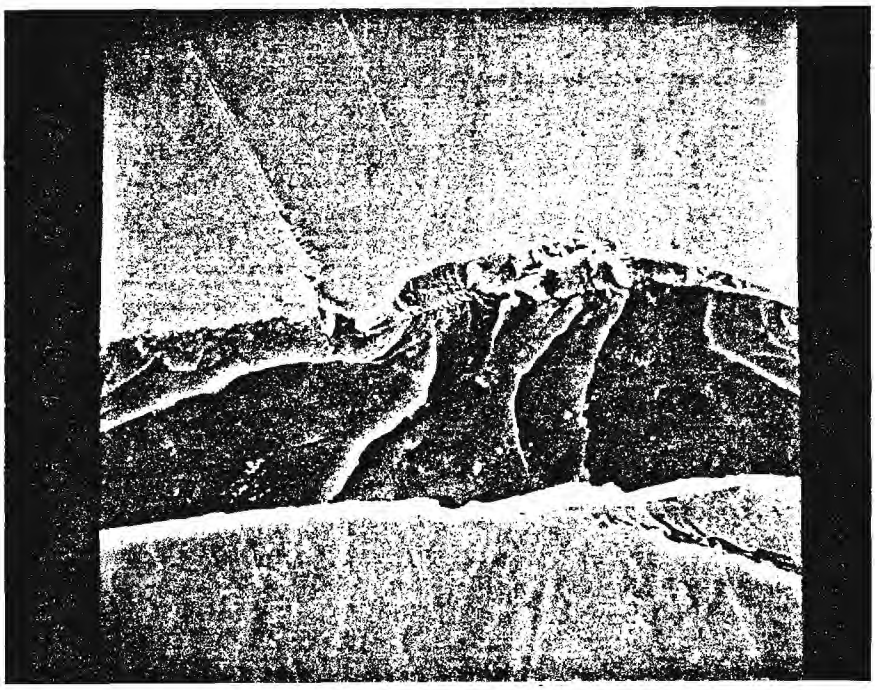

Al 520X

FIGURE 7

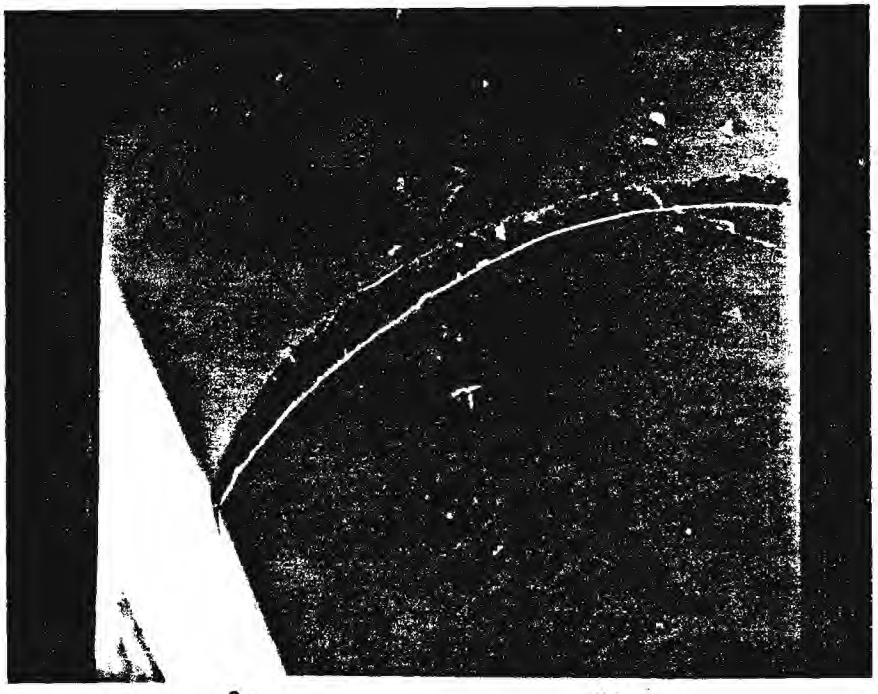

Cu 70X

Higher mag. of crack

Cu B.S. 22X

Ripples and cracks near major crack in formvar on Cu wire.

FIGURE 8

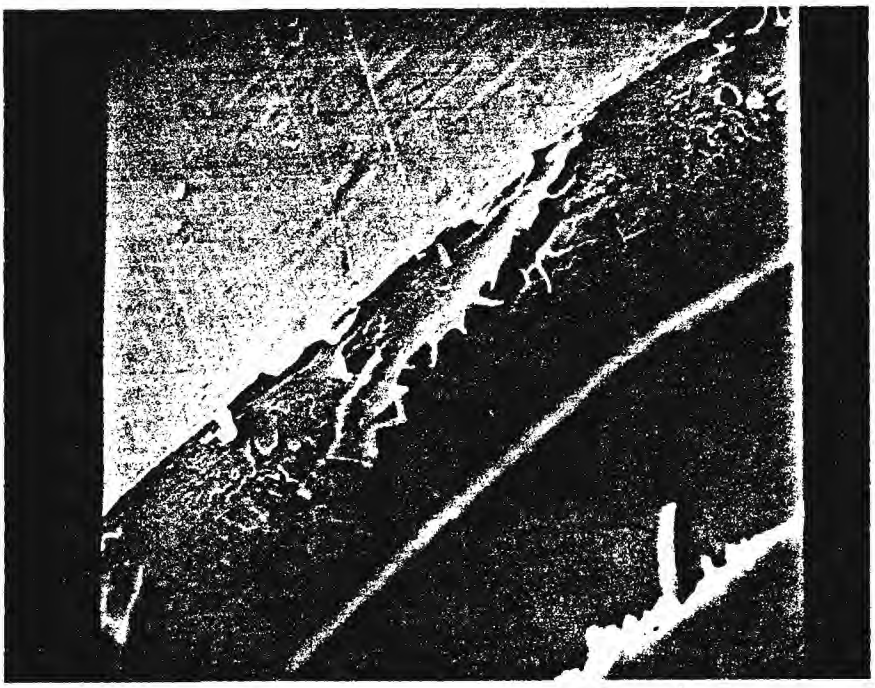

Cu 680X

Higher mag. of crack shows ductile fracture tendrils of plastic.

FIGURE 9

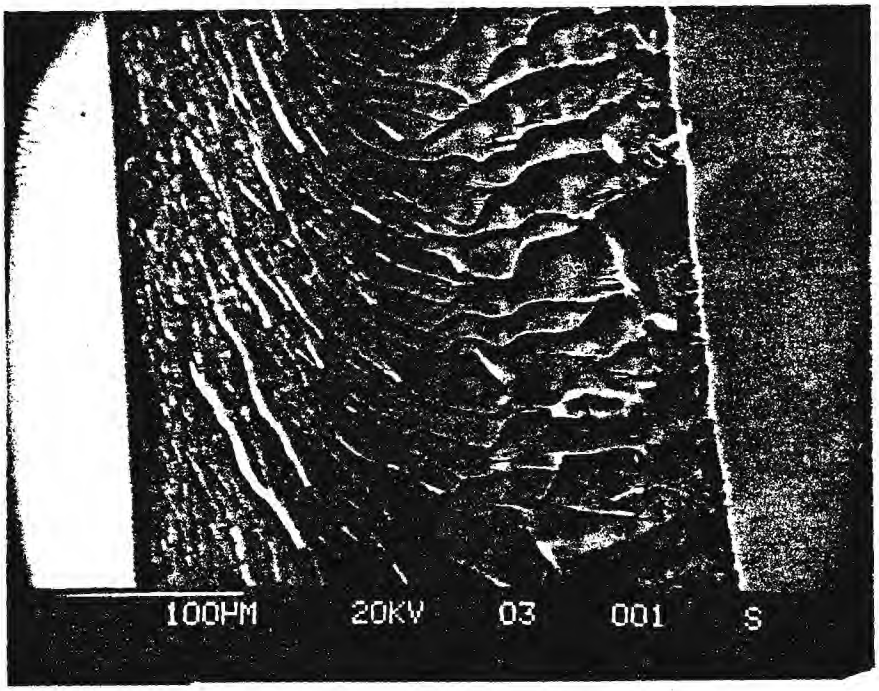

8PDG 940 250X

Dried 24 hrs. at 100°C shows brittle fracture

FIGURE 10

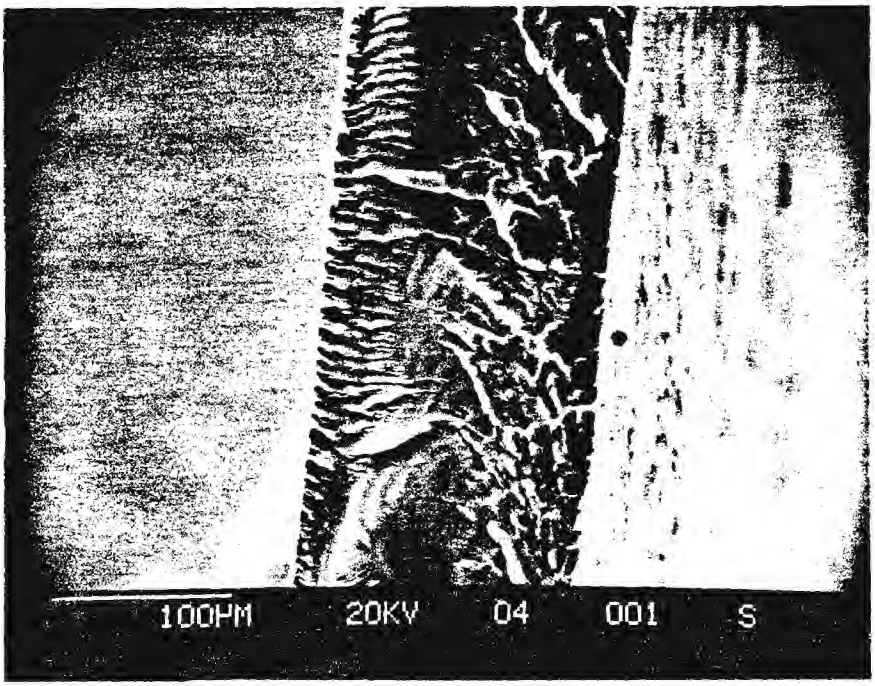

#6 544-2 250X
Dried 24 hrs. at 100°C
shows brittle fracture
FIGURE 11

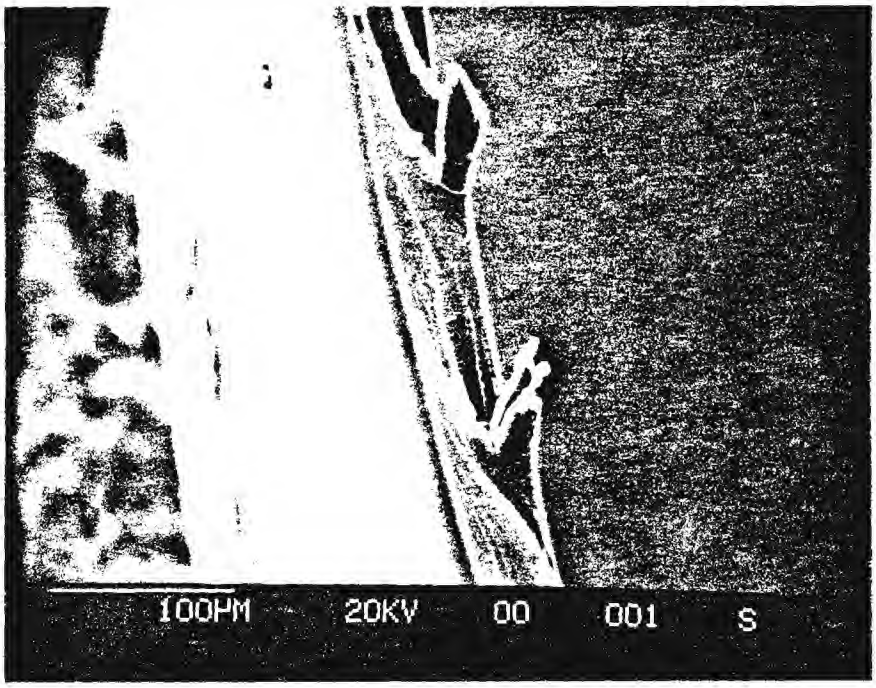

PDG 940 #5 250X
Air dried 7 days - shows
ductile fracture.
FIGURE 12

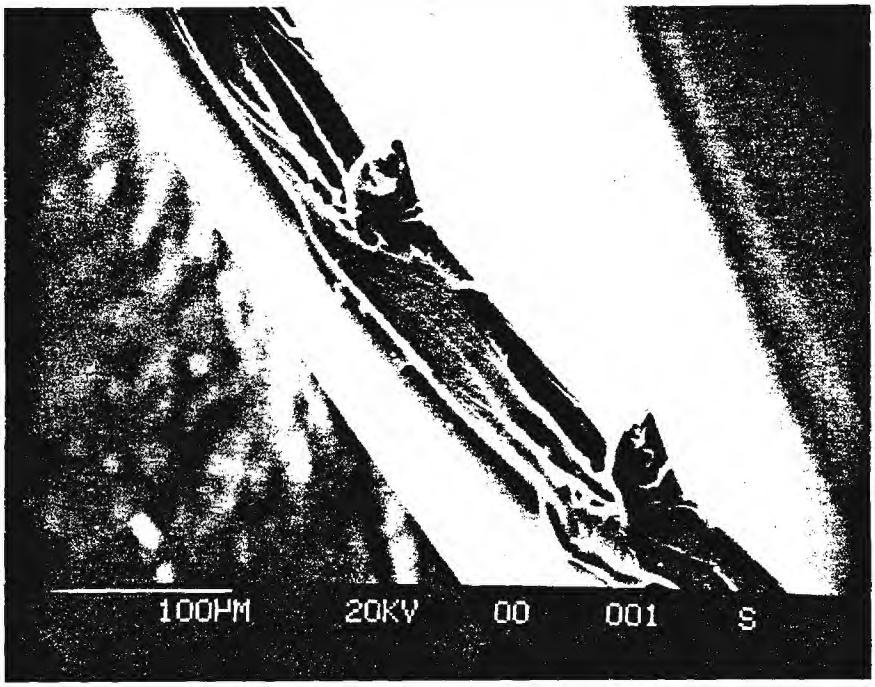

544-2 250X
Air dried 7 days - shows ductile fracture

FIGURE 13

Etching and the Morphology of Cross-Linked Polyethylene Cable Insulation

S. Bamji, A. Bulinski, J. Densley
and A. Garton

National Research Council of Canada
Ottawa, Canada

ABSTRACT

The techniques of etching by carbon tetrachloride vapor and by permanganic acid are shown to be prone to artifacts, and so earlier conclusions based on these techniques, i.e. that XLPE cable insulation has a large scale (>>10 μm) spherulitic texture structure, need to be reexamined. A comparison with XLPE film samples, where spherulite size is readily determinable by small-angle light scattering and optical microscopy, indicates that typical spherulite dimensions are <5 μm. Examination of freeze-fractured surfaces through XLPE insulation containing water-trees revealed cavities up to 10 μm diameter with no evidence of interconnecting channels. Freeze-fractured surfaces through electrical trees revealed channels several micrometers in diameter with evidence of extensive melting and polymer degradation.

INTRODUCTION

Cross-linked polyethylene (XLPE) is commonly used as the insulation of power distribution cables. Although XLPE has excellent mechanical and dielectrical properties, there is some question as to its reliability in service because of deterioration at stress concentrations or contaminants caused by high electric stress or by the combined action of moisture and electric stress. High electric stress gives rise to electrical trees which gradually penetrate the insulation eventually resulting in cable failure [1]. The combination of moisture and electric stress produces water trees, which have been shown to decrease the ac breakdown strength of cables [2]. Although several theories regarding the mechanisms of the initiation and growth of water trees have been proposed and recently reviewed by Nunes et al. [3] the detailed mechanisms of tree formation and how the water trees contribute to the final breakdown of the cable are not yet understood. The mechanisms of initiation and growth of electrical trees are also not well known and several theories have been proposed [4,5].

There has been considerable speculation about the role of polymer morphology in the initiation and growth of electrical and water trees [6-11]. For example, Wagner [6] reported that electrical trees in polypropylene followed the boundaries between spherulites. Studies of the morphology of XLPE have not yet examined the morphology in the region of either an electrical or water tree [7-9]. This paper reports the results of a study of the morphology of virgin XLPE cable insulation and also of XLPE cables containing water and electrical trees. The techniques of etching, optical and scanning electron microscopy (SEM), and small angle light scattering (SALS) were used in the investigation. To clarify the results some tests were performed on laboratory-molded thin films of low density polyethylene (LDPE), XLPE, and polypropylene (PP).

EXPERIMENTAL

The interior surfaces of 5 kV and 35 kV XLPE cables were exposed by either freeze-fracturing or cutting with a microtome and subsequent polishing with a final polish using 0.5 μm alumina powder. Freeze-fracturing using liquid nitrogen was the preferred technique because the low temperature fracture reduces the possibility of smearing structural detail, which was observed in cut and polished specimens. The polymer surfaces were then treated with different etchants in an attempt to expose morphological details.

a) the vapor of boiling carbon tetrachloride (CCl_4) for periods of 10 s to 25 min.,

b) permanganic acid (7% potassium permanganate, $KMnO_4$, in sulphuric acid) for up to one hour at room temperature, followed by washing with nitric acid or sulphuric acid [12]. The permanganic acid etching of some specimens was performed in an ultrasonic bath.

0018-9367/83/0200-0032$01.00 © 1983 IEEE

c) chromic acid (saturated $Na_2Cr_2O_7$ in sulphuric acid) for up to 24 h at 25°C,

d) nitric acid for 5 h at 72°C.

For examination in the SEM, the specimens were coated with a thin layer of gold (10 to 20 nm). Thin films of XLPE, LDPE, and PP were prepared in a hot press, etched and examined in a SEM. This allowed independent confirmation of the microscopy data, since the average spherulite size in thin films can be readily determined by SALS and optical microscopy examination. Details of the SALS technique are given elsewhere [13].

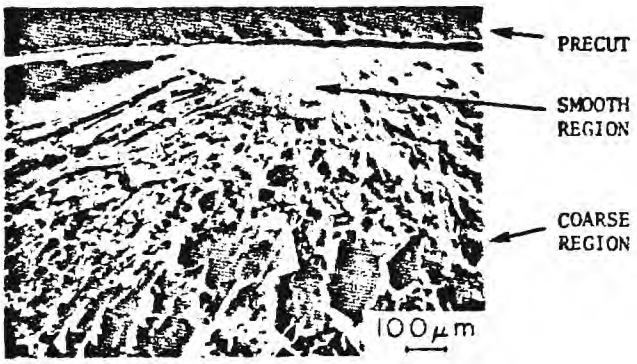

(a)

(b)

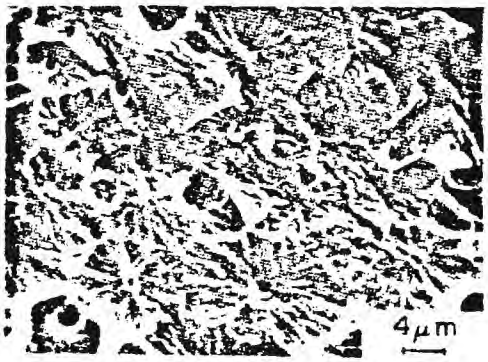

(c) Pseudo-Spherulites

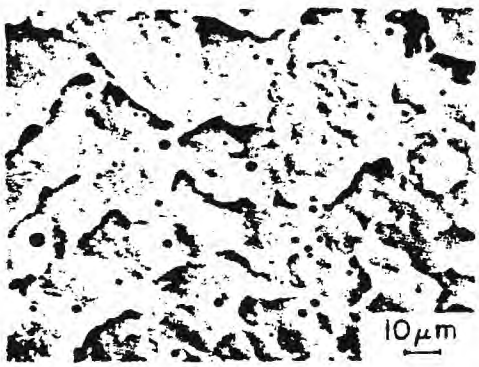

(d) Water Tree Region

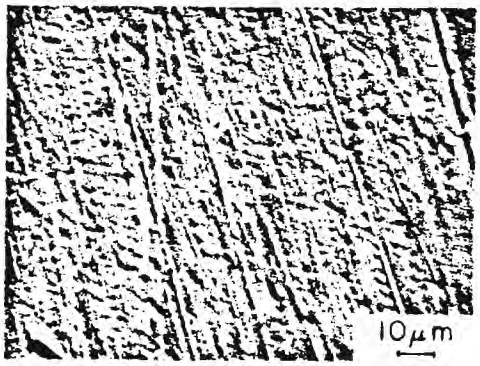

(e) Water Tree Region

Fig. 1: Typical Surfaces of XLPE Cable Insulation: (a)-(d) Freeze-fractured Surface (e) Polished Surface

RESULTS AND DISCUSSION

A. *Comparison of Freeze-Fractured and Polished Specimens*

Fig. 1 shows typical surfaces of XLPE cable insulation prepared by either the freeze-fracture technique or after cutting and polishing. To fracture the polymer in a preferred location a notch was cut in the cable prior to freeze-fracturing. At liquid nitrogen temperature, 77 K, the fracture is of a brittle type. The fractured surface consists of a relatively smooth area close to the notch followed by a coarse region. The smooth and coarse areas correspond to slow and fast crack propagation respectively [14] and give little indication of the polymer microstructure. Some fractured surfaces showed evidence of spherical structures as shown in Fig. 1c but these are probably the result of cracks spreading radially from a cavity. Wagner has reported similar artifacts and referred to them as pseudo-spherulites [15]. The region of a water tree (Fig. 1d) is characterized by a large number of cavities but there was no direct evidence of channels interconnecting the cavities. A polished surface through a water tree, Fig. 1e, shows a smaller number of cavities and also indicates distortion of the cavities during the polishing process. Electrical tree channels were also distorted and partially filled with polishing compound. Consequently most of the studies of the polymer surfaces were carried out on freeze-fractured specimens.

B. Comparison of Etching Techniques

Microscopy data obtained on etched specimens must always be treated with caution because etching may restructure the surface under examination, thereby giving a false impression of the polymer morphology.

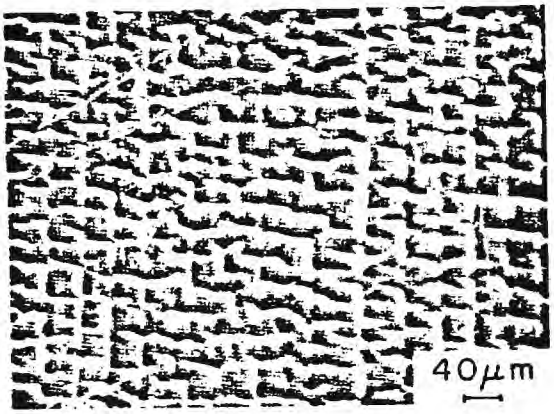

(a) 5s

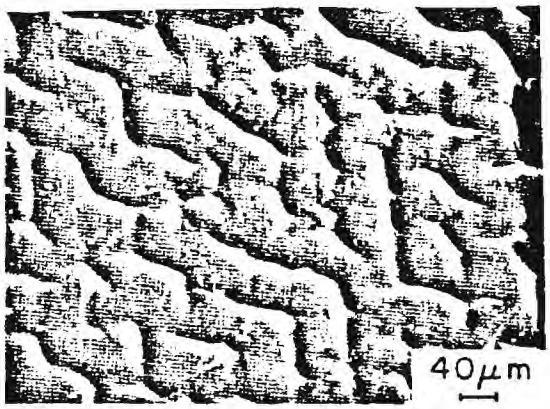

(b) 15s

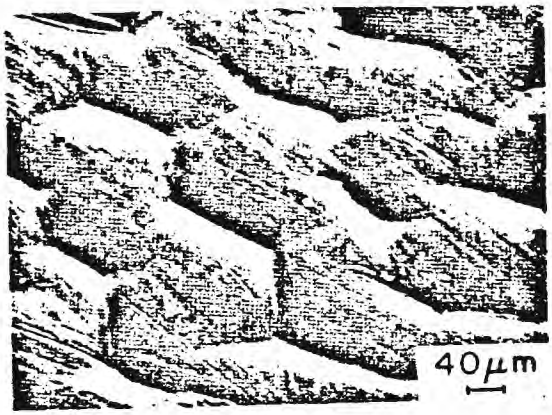

(c) 60s

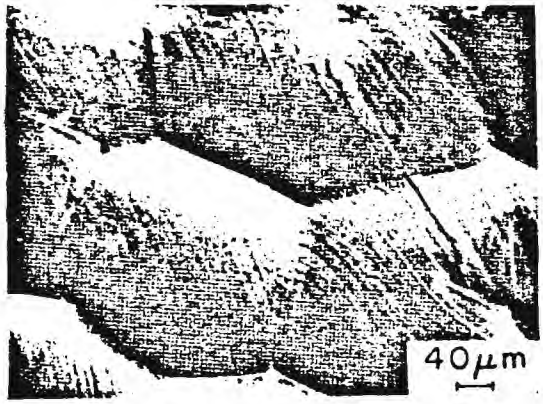

(d) 120s

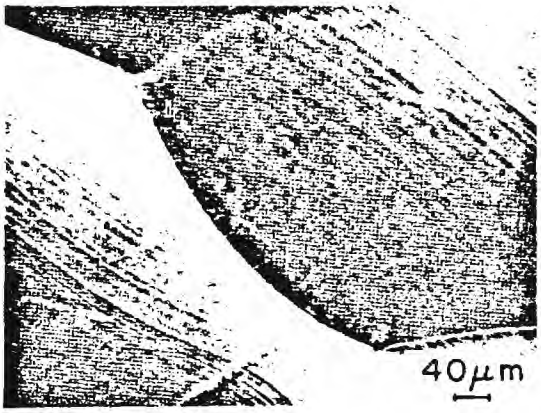

(e) 300s

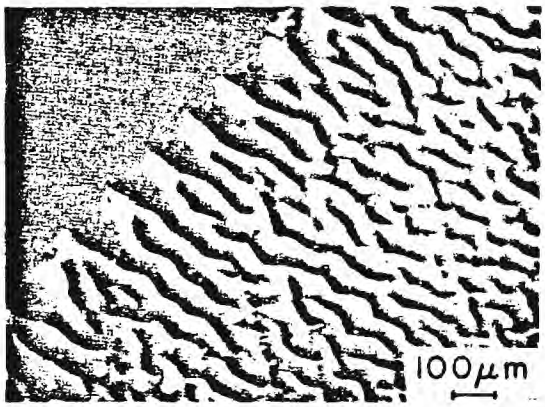

(f) 15s, Edge Effect

Fig. 2: XLPE Cable Insulation Treated in CCl_4 Vapor

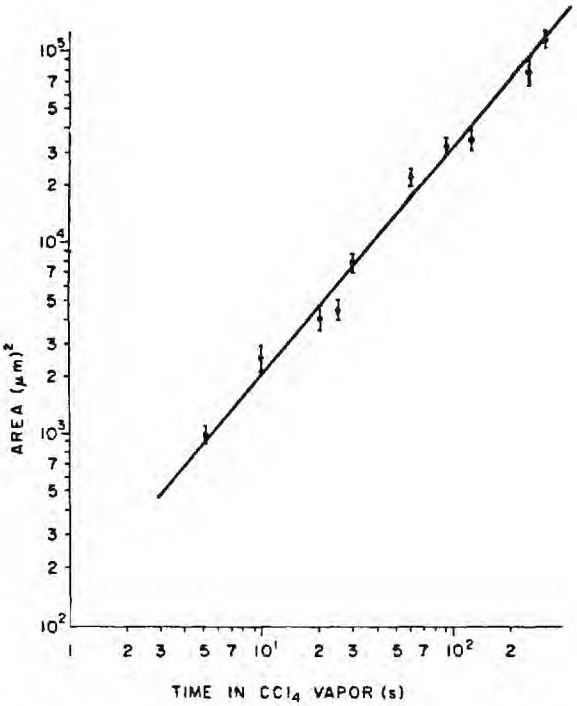

Fig. 3: Effect of Time in CCl_4 Vapor on Size of Surface Pattern.

Typical surfaces produced by CCl_4 vapor treatment are shown in Fig. 2. The polymer had a quilt-like appearance and Fig. 3 shows how the mean area of the pillowy features increases with the immersion time in the vapor. The results were calculated using a Zeiss Videoplan image analyzer. These tests were performed on specimens of similar size and thickness, all taken from the same XLPE cable. For immersion times up to 30 s, the quilt-like appearance of microtomed specimens followed the knife marks, Fig. 2a. Polished specimens showed no surface features for immersion times less than 40 s but resembled the unpolished specimens at longer times. The edges of the specimens modified the structure, the quilt-like pattern being larger around the edges. The edge effect was noted even for small sections taken from the center of the insulation, Fig. 2f. These observations imply that CCl_4 vapor treatment modifies the surface by swelling and does not expose the original polymer morphology as claimed by Phillips [7-9]. The difference between XLPE and LDPE, which softens and shows no surface structure on CCl_4 treatment, is probably their different response to swelling due to the cross-links in the XLPE.

Surfaces immersed in nitric acid or chromic acid showed increased roughness as shown in Fig. 4 but no spherulitic structure was exposed. Any scratches on the polymer surface become more pronounced with these etchants.

Permanganic acid etching of freeze-fractured XLPE revealed a distinct nodular texture, Fig. 5. The majority of the observed nodules had diameters in the range 5 to 30 μm. Some nodules had distinctive features such as spokes, Fig. 5c, rings, Fig. 5d, the small protrusions or depressions at their centers, Fig. 5b,c. It is interesting to speculate how these features relate to the morphology of the polymer if the nodules are indeed spherulites as suggested by Phillips et al. [9] and Barnes [10]. However, as will be shown below, the nodules are etching artifacts so that these additional features also are not related to the polymer morphology. Fig. 6 shows the distribution of the equivalent circle diameter of the nodules calculated using the image analysis system, for etched, 5 kV XLPE insulation. The mean diameter was 20.3 μm with minimum and maximum values of 6.8 μm and 47.5 μm respectively. Similar results were obtained with freeze-fractured surfaces of LDPE cable insulation.

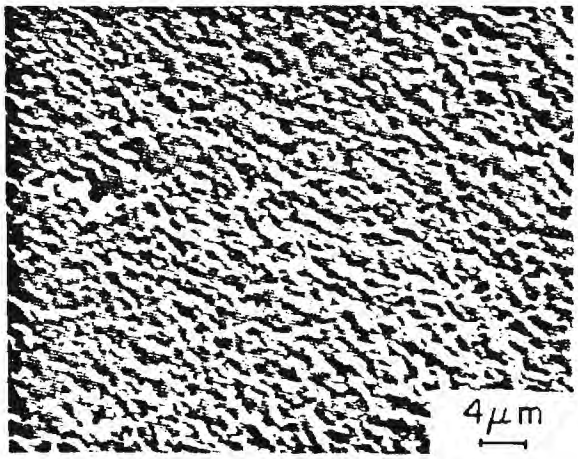

(a) Nitric Acid

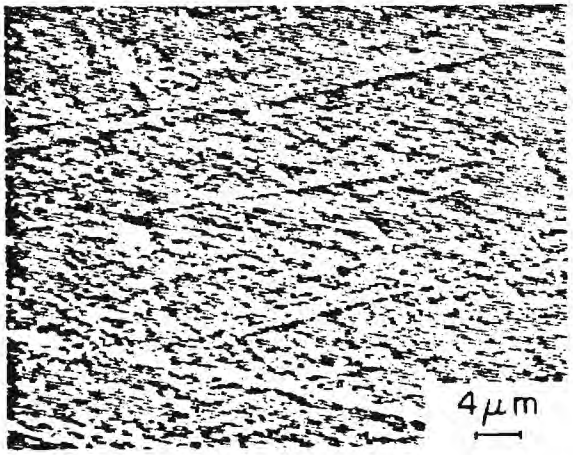

(b) Chromic Acid

Fig. 4: Surfaces of XLPE Etched in Nitric and Chromic Acids

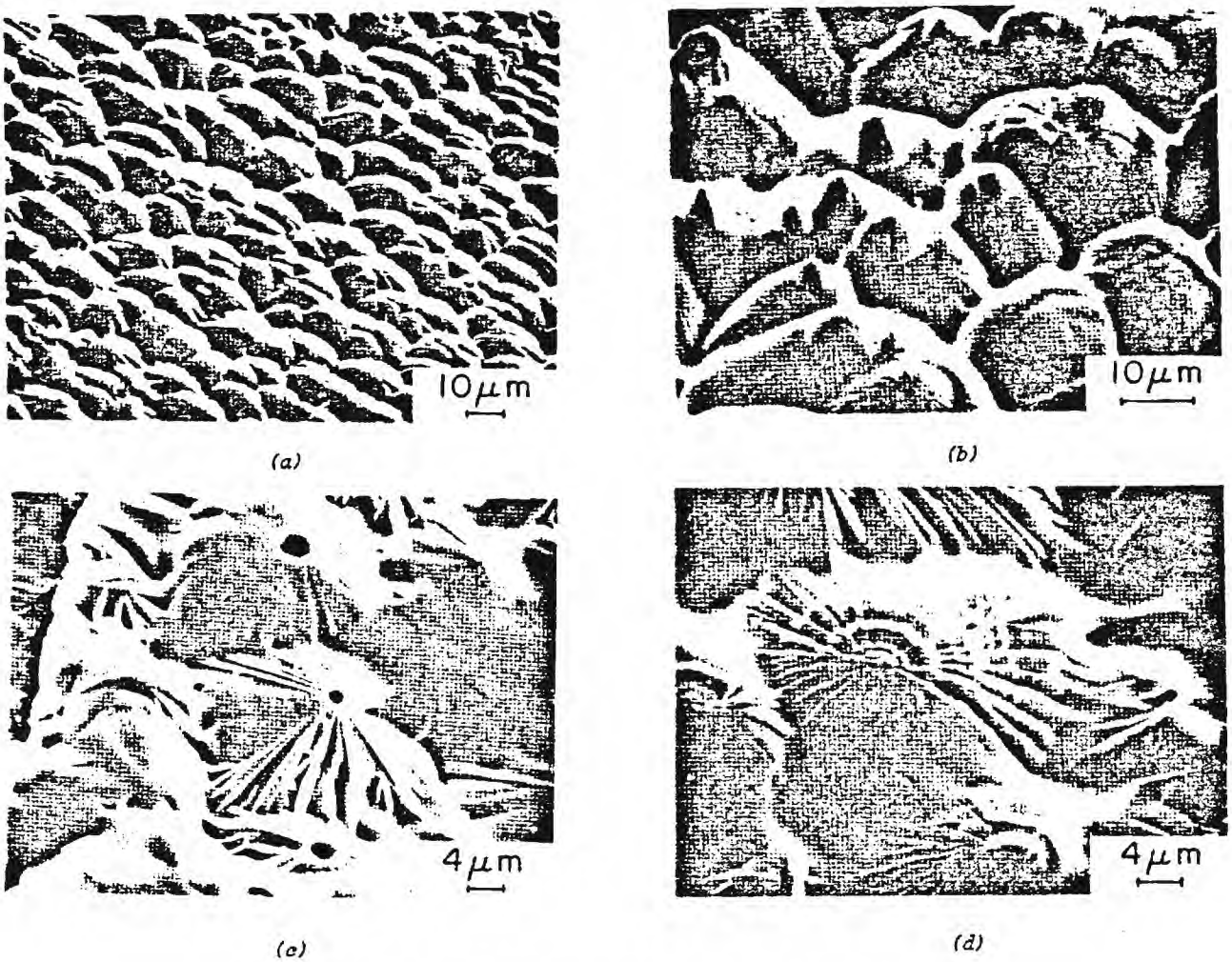

Fig. 5: Permanganic Acid Etch of Virgin XLPE

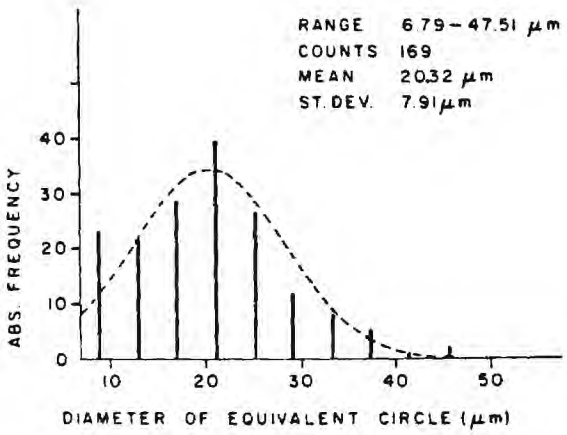

Fig. 6: Distribution of Nodule Size for 5 kV XLPE Cable

Etching in the presence of ultrasonic agitation tended to produce a more uniformly etched surface but did not change the nodule dimensions.

The effect of time of immersion in the permanganic acid was also studied using freeze-fractured sections of 35 kV XLPE cable insulation. The results are listed in Table 1.

The results show that there is no consistent variation in the nodule size with duration of etching and that the size of the nodules are highly variable even within one sample. No consistent variation in the nodule size with insulation radius was observed for any cable of insulation thickness between 0.75 and 10 mm.

Etching of XLPE Containing Water Trees or Electrical Trees

Because the permanganic acid etched surface revealed interesting features which have been interpreted by others as being spherulites, sections of cables containing water or electrical trees were etched to determine if there was any relationship between the trees and the surface features. A typical unetched surface containing water trees is shown in Fig. 1d.

TABLE 1

Duration of Etching Minutes	Nodule Size (Equivalent Circle Diameter) Mean ± C.I.* µm	Range µm
10	17.7 ± 1.4	12 - 25
20	12.5 ± 1	5 - 22
30	21.9 ± 2	15 - 40
40	29.2 ± 5	16 - 59
60	15.3 ± 2	4 - 32

*95% Confidence Interval

The treed region contained a large number of cavities ranging from 0.8 to 9.8 µm, the average of over one hundred measurements being 3.1 µm. Other water-treed regions were also examined and the results are shown in Table 2.

Sections along and normal to the tree axis were studied with no evidence of channels interconnecting the cavities. The resolution was better than 0.1 µm diameter. The permanganic acid etched surface of a section through a water tree shows both cavities and nodules, Fig. 7. The most important observation was that the distribution of the cavities was independent of the nodules, with cavities occurring at the centers of nodules, within the spokes and also at the boundaries. The etching did not reveal any interconnecting channels between the cavities.

Freeze fracture through an electrical tree grown in 35 kV XLPE cable insulation in the laboratory clearly shows tree channels, which vary in diameter up to about 10 µm, Fig. 8a. The density of the tree channels depends on the applied voltage, frequency and temperature [1]. Fig. 8 also shows a permanganic acid etched specimen containing an electrical tree. The discharge channels do not follow the nodule boundaries as might be expected if the nodules were true spherulites and considering the results of Wagner for polypropylene [6]. The nodules are smaller in diameter in the region of a breakdown channel and also tend to be aligned along the tree channels, Fig. 8c.

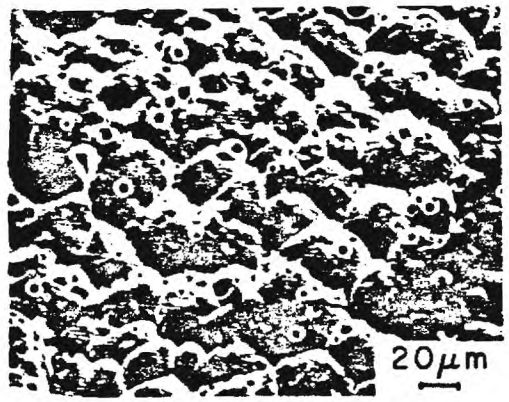

(a)

(b)

Fig. 7: Etched, Freeze-fractured Sections through Water Tree, 5 kV XLPE Cable

TABLE 2

Specimen No.	Average Diameter µm	Void Density Number/mm^2	% Area Occupied by cavities %	Surface Condition
1	1.6	1.6×10^4	3.3	not etched
2	2.9	0.6×10^4	2.9	etched
3	1.5	1.4×10^4	2.6	not etched
4	-	0.6×10^4	-	etched
5	-	13.5×10^4	-	not etched

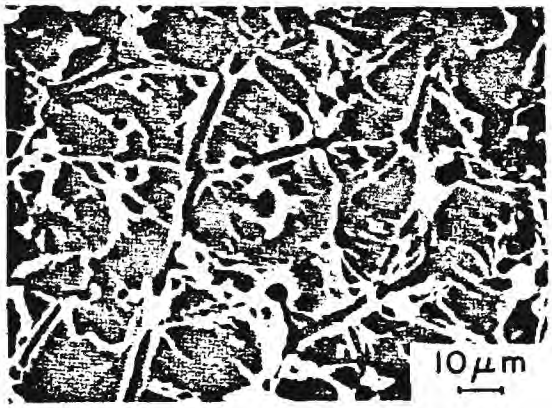

(a) Un-etched

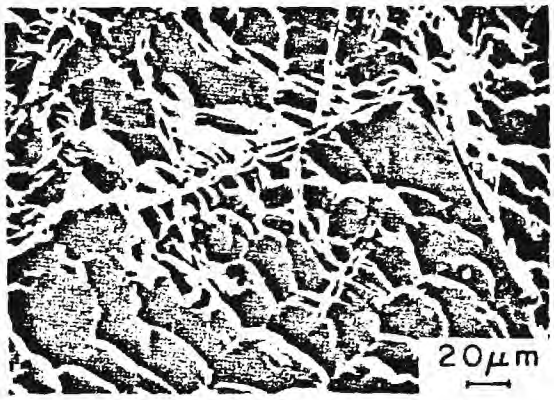

(b) Etched

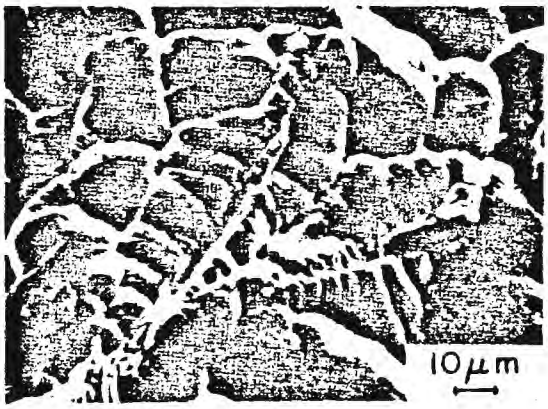

(c) Etched

(d) Etched

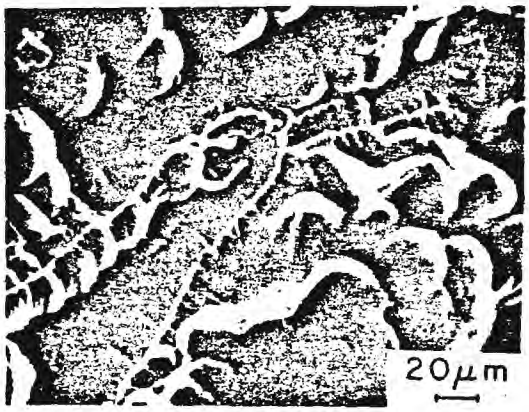

(e) Etched, Remote from Tree

Fig. 8: Freeze-fractured Sections through an Electrical Tree, 35 kV XLPE Cable

Tests on Film Specimens

To confirm whether permanganic acid etching reveals the true polymer morphology, some tests were performed on thin films, 20 μm, of LDPE, XLPE, and PP, the morphology of which could be checked using SALS and optical microscopy. Thin films of these materials were molded in the laboratory and the spherulite size controlled by the thermal treatment given the films. The results for a XLPE film are shown in Fig. 9. The film was etched in permanganic acid for 20 minutes before examination in an optical microscope with non-polarized light (Fig. 9a). Fig. 9b shows the same region as Fig. 9a under polarized light. Many spherulites about 4 μm diameter can be seen inside the larger nodular structures on the surface of the etched specimen. Similar sized spherulites were observed in an unetched film. The average diameter as measured by SALS was 4.8 μm, in agreement with the measurements using polarized light and the optical microscope, and smaller than the nodules produced by etching. Similar results were observed for LDPE.

The distribution of the nodule diameters, measured with an image analyzer, is shown in Fig. 10. The mean value of 290 measurements is 10.9 μm with minimum and maximum diameters of 4.5 μm and 17.6 μm respectively.

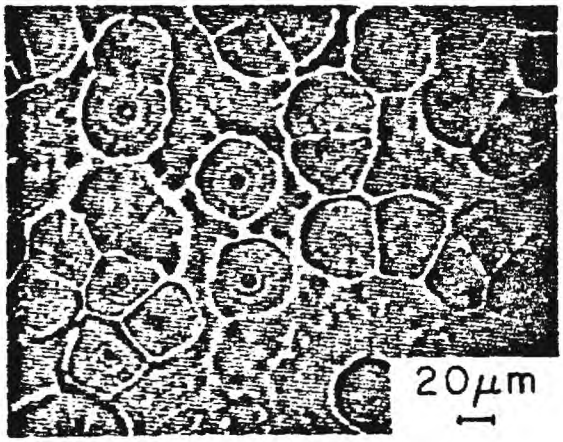

(a) Non-Polarised Light

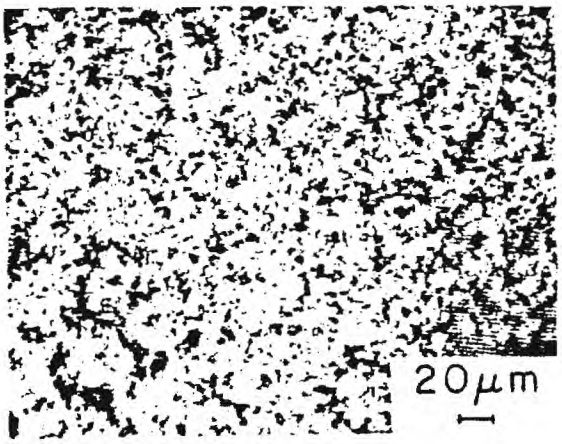

(b) Polarized Light same as Region (a)

Fig. 9: Permanganic acid etched XLPE film, (optical microscope)

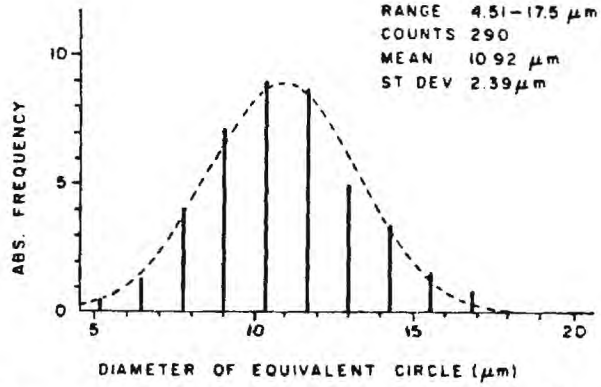

Fig. 10: Distribution of nodule size of XLPE film

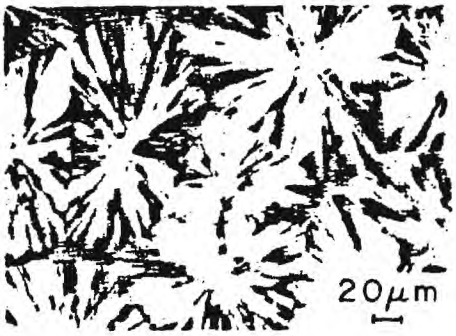

(a)

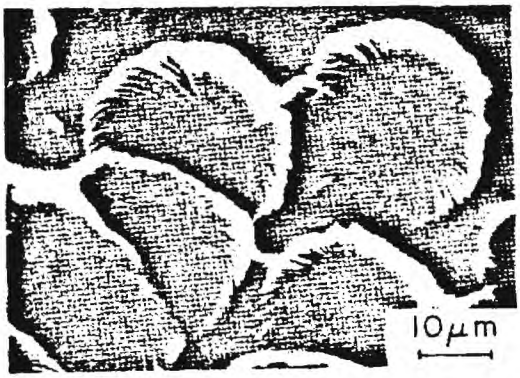

(b)

(c)

Fig. 11: Micrographs of PP and XLPE Film
(a) PP film, polarized light, unetched
(b) PP film, permanganic acid etched (SEM)
(c) XLPE film, permanganic acid etched (SEM)

The tests were repeated on PP film which was cooled sufficiently slowly to produce large spherulites as shown in Fig. 11a. The etched surface, shown in Fig. 11b, contained nodules of similar size to those for XLPE film, Fig. 11c. Fig. 12 shows the distributions of the equivalent circle diameters of the spherulites, as measured by optical microscopy, and of the nodules. The mean diameters of the spherulites and nodules were 100 and 16.3 μm, respectively, with the spherulites ranging between 37 and 210 μm and the nodules between 5 and 31 μm. These results confirm that the

nodules revealed by the permanganic acid etching are artifacts and are not related to the true spherulite structure of the polymer. It should be noted that the true spherulites were not measured in the XLPE cable insulation due to the difficulty in obtaining a polished thin section suitable for examination by polarized light. However, because of the similarities in the surface features of the etched XLPE cable and XLPE film specimens, it is reasonable to assume that the nodules on the cable specimen surfaces are also artifacts and do not represent morphological details.

It can be argued that the examination of molded films may be misleading because the polymer morphology contacting the mold surfaces (in this case, glass), may differ from the bulk, with the inference that the nodular texture observed in the etched film may be truly spherulitic but exists only on the surface. This argument is invalid for several reasons. The nodular texture almost disappears when viewed between crossed polarizers. Fig. 9b was also taken at the same settings of the microscope as Fig. 9a except for the addition of the crossed polarizers, and since the depth of focus of an optical microscope at these magnifications is poor (<5 μm) the nodules (Fig. 9a) and the spherulites (Fig. 9b) both exist on or near the film surface. Finally, examination of polypropylene film specimens shows that the nodular texture is independent of the average spherulite size and thermal history of the specimen which would be surprising if the nodules were indeed spherulites.

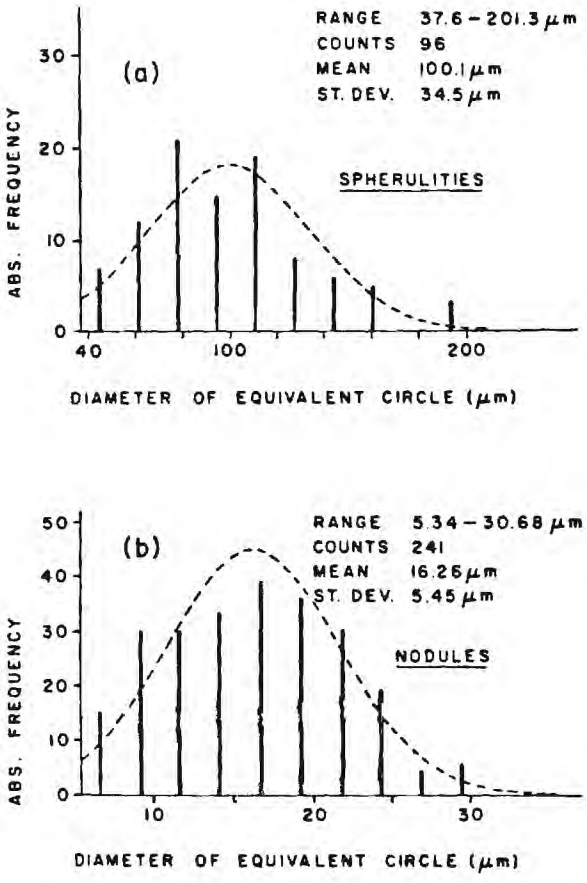

Fig. 12: Distribution of Spherulite and Nodule Sizes for PP Film.

One can only speculate upon the origin of the nodular artifacts. A reasonable explanation is that regions of swollen, partially dissolved, polymer collapse when the etchant is removed by washing. This hypothesis is supported by the observation that the nodular texture is distinctly different in size in the area of cracks or scratches on the specimen Fig. 8e. The nature of the collapsed structures must be influenced by the chemical and physical structure of the polymer (e.g. note smaller nodules along electrical tree channels, Fig. 8d) but cannot be said to represent structural detail in the unetched polymer.

CONCLUSIONS

Carbon tetrachloride vapor produces a quilt-like surface texture for XLPE which varies with time of exposure to the vapor. This results from swelling of the surface and does not correspond to the original polymer morphology.

Etching by nitric acid or chromic acid roughens the surface of the polymer but does not reveal any spherulitic structure.

Permanganic acid etching of XLPE cable insulation produces a well defined nodular texture, with the diameters of the nodules up to 30 μm. The nodule dimensions showed no consistent variation with insulation thickness (0.75 to 10 mm) and cable manufacturer. Permanganic acid etching of thin films of XLPE, LDPE, and PP also produces this nodular texture. Polarized light, via microscopy or SALS, however, reveals the true spherulites in these films. The spherulites are different in size from the surface nodules, and independent of them. The spherulite sizes, as expected, varied with the polymer and its thermal history. These observations on film specimens indicate that the nodules produced by permanganic acid are artifacts of the etching process. The similarity in the surface features of the etched XLPE cable and the film specimens suggests that the nodules on the surface of the cable specimens are also artifacts and do not represent morphological details of the polymer.

The location of cavities in the region of a water tree is independent of the nodular texture, with no preference for the cavities to be located at the boundaries. The cavities were up to 10 μm diameter with no evidence of interconnecting channels. The cavity density was of the order of $10^4/mm^2$ of surface area. Electrical trees also grow independent of the nodular texture although nodules are smaller within a breakdown channel than those remote from it. This is probably due to the degradation which occurs in the channels due to partial discharges.

REFERENCES

[1] J. Densley, "An Investigation into the Growth of Electrical Trees in XLPE Cable Insulation", IEEE Trans. Elect. Insulation, EI-14, pp. 148-158, June 1979.

[2] A. Bulinski and J. Densley, "The Voltage Breakdown Characteristics of Miniature XLPE Cables Containing Water Trees", IEEE Trans. Elect. Insul., EI-16, pp. 308-316, August 1981.

[3] S. L. Nunes and M. T. Shaw, "Water Treeing in Polyethylene - A Review of Mechanisms", IEEE Trans. Elect. Insul., EI-15, pp. 437-450, December 1980.

[4] R. M. Eichhorn, "Treeing in Solid Extruded Electrical Insulation", IEEE Trans. Elect. Insul., EI-12, pp. 2-18, Feb. 1976.

[5] G. Bahder, T. W. Dakin and J. H. Lawson, "Analysis of Treeing Type Breakdown", CIGRE 1974, Report 15-05.

[6] H. Wagner, "The Influence of Superstructures on the Electrical Breakdown of Partially Crystalline Polymers", 1974 Annual Report Conference on Electrical Insulation and Dielectric Phenomena, pp. 62-70, 1975.

[7] P. J. Phillips, "Identification and Location of Microscopic Inorganic Impurities in Cable Insulation", IEEE Trans. Elect. Insul., EI-13, pp. 451-453, December 1978.

[8] J. Muccigrosso and P. J. Phillips, "The Morphology of Cross-Linked Polyethylene Insulation", IEEE Trans. Elect. Insul., EI-13, pp. 172-178, June 1978.

[9] D. V. Brower, K. L. Naylor and P. J. Phillips, "Multiple Morphologies in Cross-Linked Polyethylene" 1980 Annual Report Conference on Electrical Insulation and Dielectric Phenomena, pp. 113-122, 1980.

[10] S. R. Barnes, "Morphology of Cross-Linked Polyethylene", Polymer, 21, pp. 723-725, 1980.

[11] S. M. Kolesov, "The Influence of Morphology on the Electric Strength of Polymer Insulation", IEEE Trans. Elect. Insulation, EI-15(5), pp. 382-388, 1980.

[12] R. H. Olley, A. M. Hodge, and D. C. Bassett, "A Permanganic Etchant for Polyolefins", Journal of Polymer Science, Polymer Physics Education, 17, pp. 627-643, 1979.

[13] A. Garton, D. J. Carlsson, R. F. Stepaniak, and D. M. Wiles, "The Use of Small-Angle Light Scattering (SALS) to Examine the Structure of Fibres', Textile Research Journal 49, pp. 335-342, June 1979.

[14] H. H. Kausch, Polymer Fracture, Vol. 2 of Series Polymers/Properties and Applications, Springer Verlag, 1978, pp. 293.

[15] H. Wagner, "Pseudo-Spherulite Structures in Cross-Linked Low Density Polyethylene", IEEE Trans. Elec. Insulation, EI-13, pp. 81-86, April 1978.

Manuscript was received 3 March 1982.

A-3507-000

ENGINEERING EXPERIMENT STATION
Georgia Institute of Technology
A Unit of the University System of Georgia
Atlanta, Georgia 30332

October 19, 1983

Mr. Richard Buckley
Manager Materials Development
Westinghouse Electric Company
Newton Bridge Road
Athens, Georgia 30601

Attention: Mr. Buckley

Subject: P.O. No. 76-37262-S

Enclosed is the final report on "Transformer Insulation Failure". We believe that the overall research efforts will enable Westinghouse to have a better understanding of the insulation characteristics. From a personal view we both have had an opportunity to learn from each other.

Sincerely yours,

Wallace Shakun, Ph.D.
Industry Programs Office
Energy and Materials
Sciences Laboratory

WS:gb

cc: L.W. Mesta
Purchasing Agent, Westinghouse

ENGINEERING EXPERIMENT STATION
Georgia Institute of Technology
A Unit of the University System of Georgia
Atlanta, Georgia 30332

October 18, 1983

M E M O R A N D U M

TO: W. Shakun

FROM: J. W. Gooch

SUBJECT: "Transformer Insulation Failure", Westinghouse Electric Company, Athens, GA

We have finished the analyses of two wire coatings for the Westinghouse Electric Company, Athens, Georgia. The results of these analyses are contained in the following paragraphs.

Curing of Coatings

The Formvar^{R} resins were coated on aluminum panels (4" X 6") with a Baker^{R} Draw-Down Blade. The wet film thickness was four mils. The Formvar^{R} coatings, nos. 544-2 and PDG-940, were cured at 100°C for 15 Sec., then 370°C for 15 Sec. This curing procedure was obtained from Mr. Richard Buckley of Westinghouse via telephone on September 2, 1983.

The coated aluminum substrates were cured at the above temperatures in our Thermolyne 1400 furnace.

Adhesion

Adhesion tests were performed on the coated aluminum substrates. Adhesion was determined by the Elcometer Adhesion Tester and the Tape Test Method. (ASTM D 3359-78). The results are contained in Table 1. It can be seen from

Coating	Elcometer Adhesion, p.s.i.	ASTM D 3359-78
544-2	50	4
PDQ-940	60	3

Table 1 that the PDG940 coating possesses better adhesion by "pulling" the coating, but demonstrates less adhesion and brittleness by the Tape Test Method.

Hardness

Panel hardness testing was performed on the above coatings by ASTM D 3363-74. The results are contained in Table 2. It can be seen from Table 1 that the hardness of

Table 2

Trial	Hardness	
	544-2	PDQ-940
1	H-5	H6+
2	H-6	H6+
3	H-5	H6
4	H-6	H6+
5	H-6	H6
6	H-5	H6

PDG-940 is H6 to H6+ and the hardness of 544-2 is H5 to H6. This means that PDG-940 is harder than 544-2.

Thermal Properties

Differential Scanning Colorimetry (DSC), Perkin Elmer Model DSC1, curves were generated from the above coatings. The temperature range was 25°C to 504 C and the scan rate was 20°C/min. These curves indicated significant differences between the above coatings with respect to thermal transitions such as melting. The 544-2 coating demonstrated a consistent positive sloping curve with temperature from 105°C as shown in Figure 1. This means that the coating continuously softened and melted with increasing temperature. The PDG-940 demonstrated a transition at 125°C, but remained stable to 230°C. Referring to Figure 2, after 230°C a continuous positive slope in the curve was demonstrated to 405°C. These

DSC curves demonstrate that the PDG-940 coating is more densely crosslinked.

Relative Molecular Weight of Components

Relative molecular weights of the above uncured resins were analyzed by gel permeation chromatography (GPC). Figures 3 and 4 represent 544-2 and PDG-940, respectively. It can be seen from a comparison of Figures 3 and 4 that a higher molecular weight fraction exists at about retention time 24 to 27 for PDG-940. We do not know which component of the resin formulation corresponds to this higher molecular weight fraction. This would require further analysis.

Chemical Structure Identification

Both of the above resins were analyzed with infrared spectroscopy in the "neat" and dried forms. In the neat form, the liquid samples were placed between AgCl disks. In the dried form, solvent was removed at 105°C under vacuum for three hours and the dried film was analyzed. Observing Figure 5, it can be seen that the spectra of 544-2 and PDG-940 was very closely related with no significant differences. The solvents are present in these spectra and they are similar. Also, the dried films of each resin are similar as observed in Figure 6. Except for the possible presence of contaminants below 2% in volume, the chemical structure of these materials are similar.

Percent Non-Volatile

The percent non-volatile content of 544-2 and PDG-940 were determined by ASTM D 115-72. The results are 31.3% and 32.0% for 544-2 and PDG-940, respectively.

Conclusions

From the above analyses the following conclusions were drawn:

1) The chemical structure of 544-2 and PDG-940 are similar.
2) The percent non-volatile content of 544-2 and PDG-940 are similar.
3) The hardness of 544-2 and PDG-940 are different and the PDG-940 is significantly harder.
4) The adhesion on 544-2 and PDG-940 are different and the PDG-940 possesses greater "pull" adhesion, but lower "tape test" adhesion. PDG-940 appears to be brittle.
5) The thermal properties of 544-2 and PDG-940 are different. PDG-940 softens less with temperature,

and this is due to a greater degree of crosslinking which is expected with increased hardness.

6. The molecular weight of 544-2 and PDG-940 are different. PDG-940 possesses a higher molecular weight at about 24 to 27 units retention time. This constitutes a formulation difference.

Summary

A formulation difference exists between 544-2 and PDG-940. The difference is a higher molecular weight for one or more of the components in Figure 4 compared to those in Figure 5. Thermal stability curves further show evidence of a denser more crosslinked PDG-940 material compared to 544-2 material. Hardness further shows that PDG-940 is a different material.

From our understanding, the failure mode was fracture of the insulation (coating) on the wire when compressive forces were applied to the PDG-940 material. Whereas, the 544-2 material performs satisfactorily. We conclude that the PDG-940 insulation coating is more brittle and does not possess sufficient flexibility. This is due to a formulation different in at least one of the components. A thorough chemical analysis would be necessary to determine the exact chemical composition of these materials.

Figure 1. 544-2 Differential Scanning Colorimetry Curve.

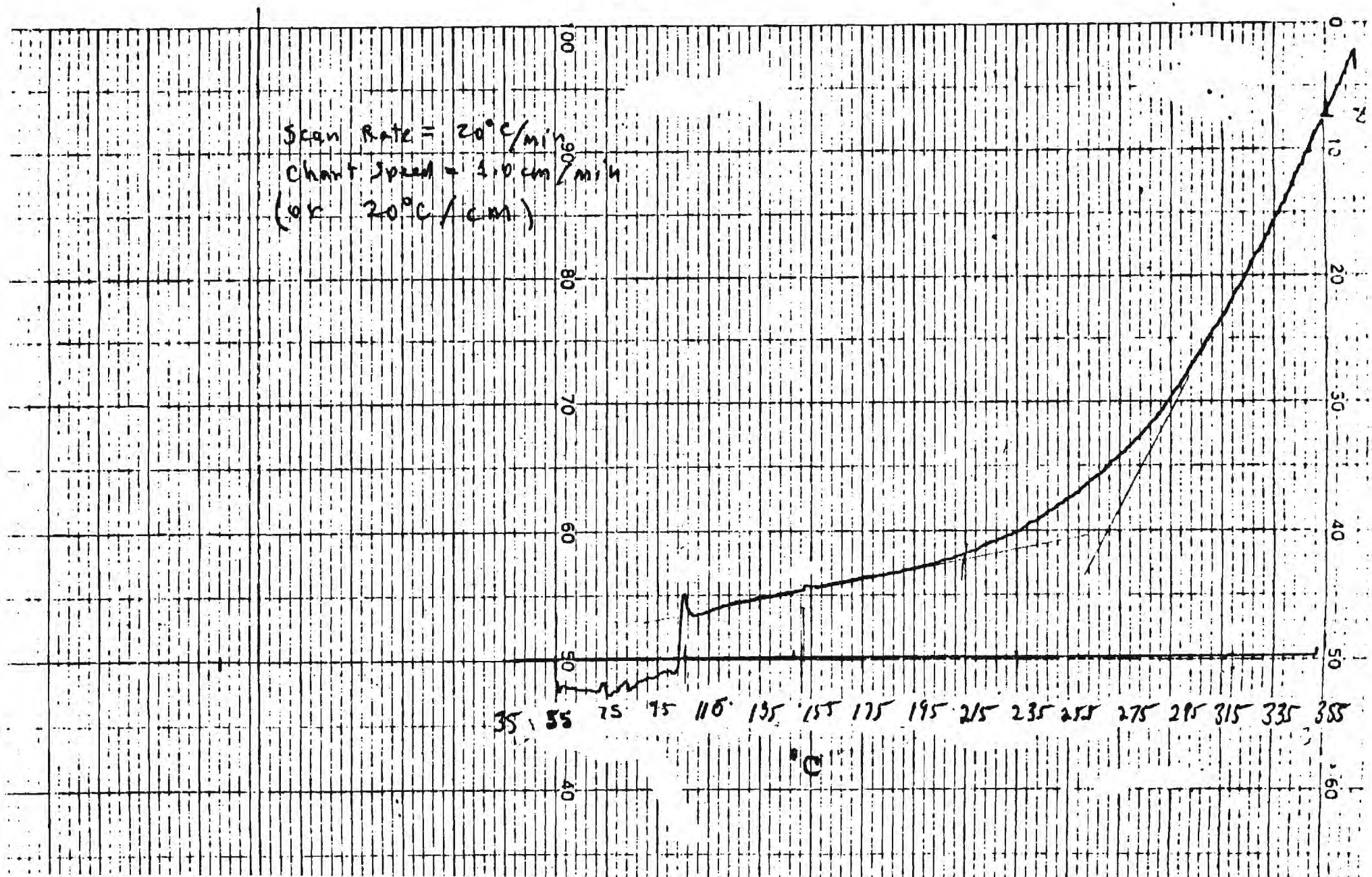

Figure 2. PDG-940 Differential Scanning Colorimetry Curve.

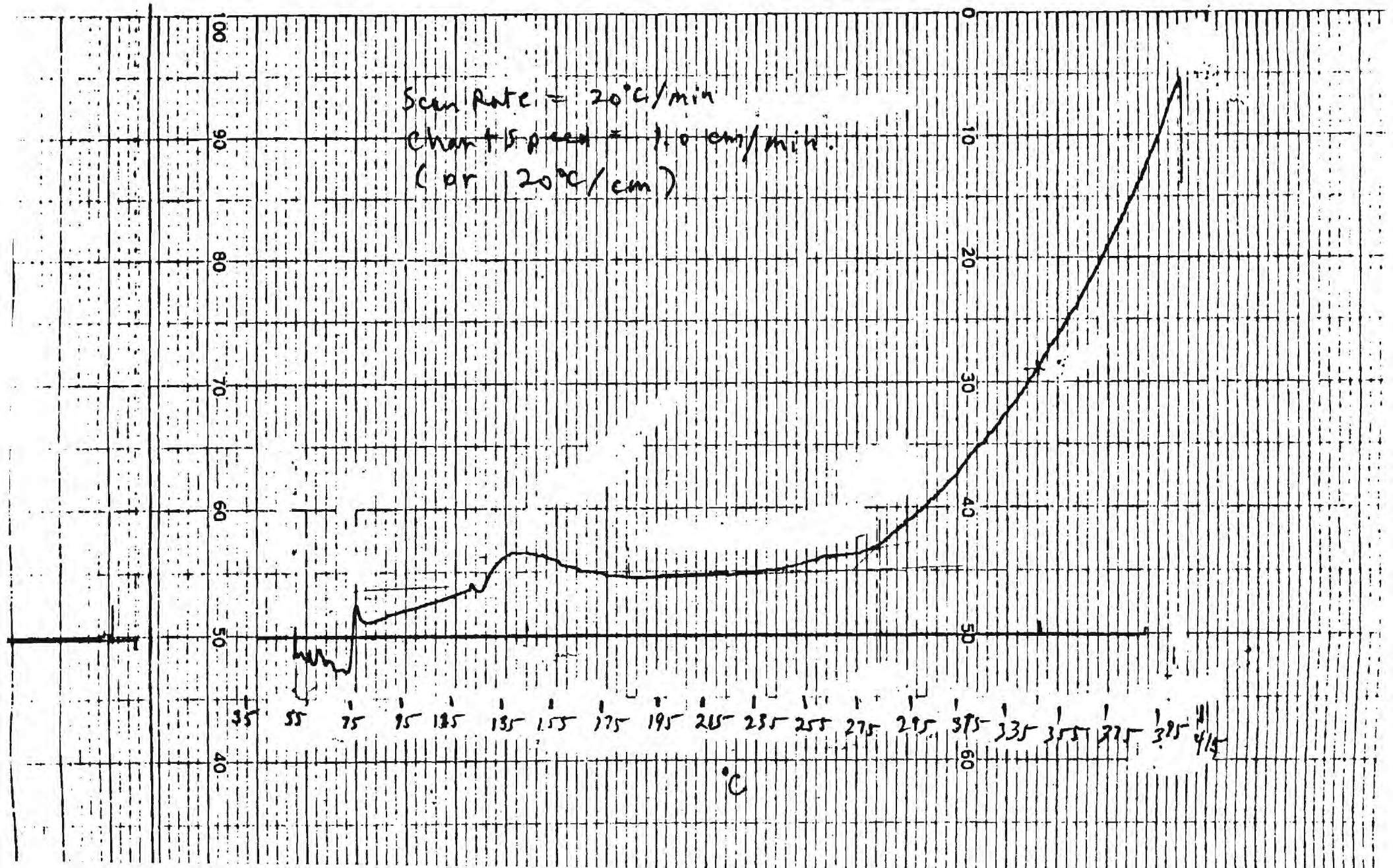

544-2
B2942

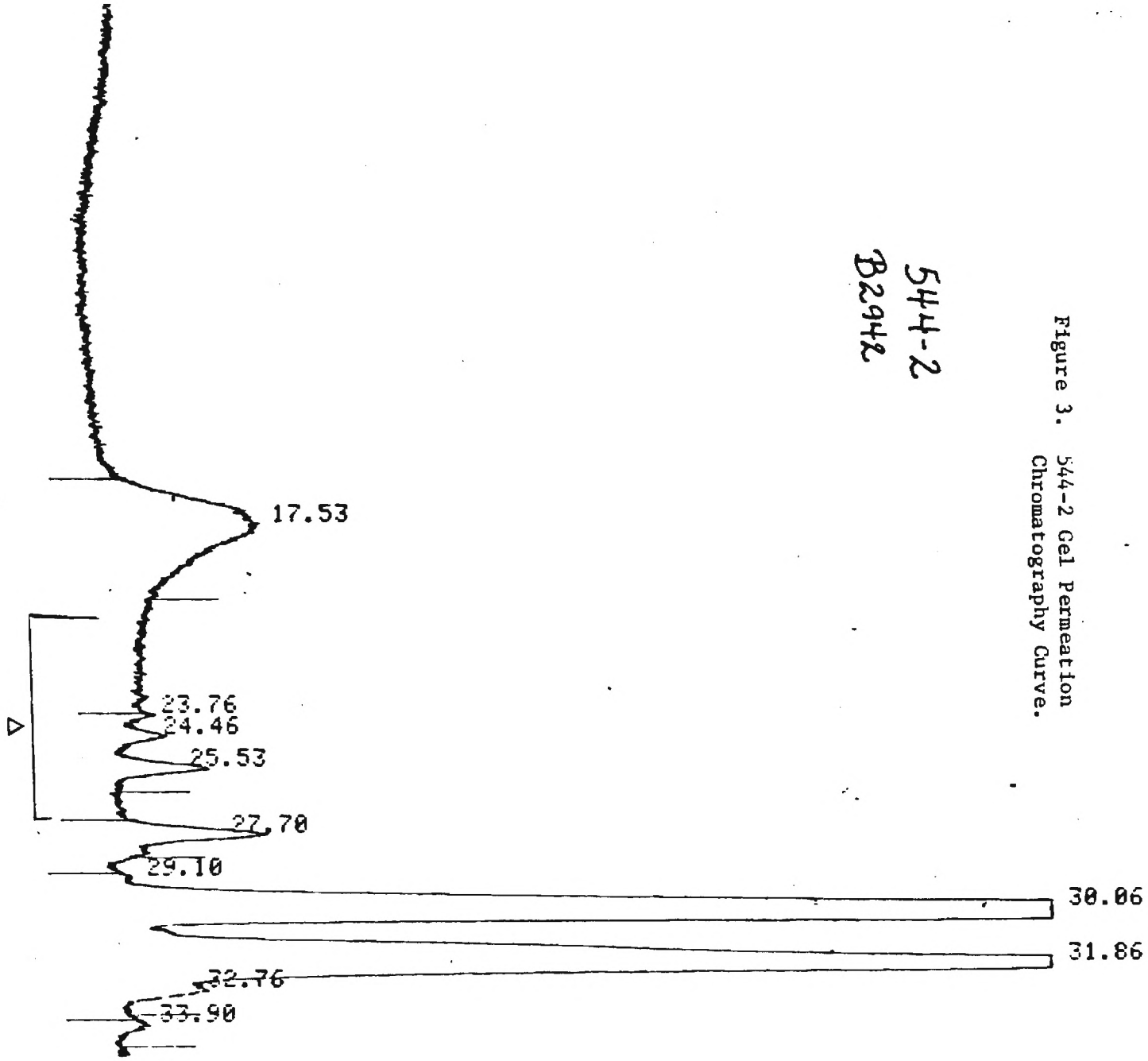

Figure 3. 544-2 Gel Permeation Chromatography Curve.

JUN. 12, 1983 15:22:44 CHART 0.50 CM/MIN
RUN #6 CALC #0
COLUMN SOLVENT OPR ID: 6

EXTERNAL STANDARD QUANTITATION

PEAK#	AMOUNT	RT	EXP RT	AREA		RF
	368389.00000	17.53		368393615	L	0.000000E0
	2089.81000	23.76		2089820	F	0.000000E0
	4990.81000	24.46		4990829	F	0.000000E0
	18660.50000	25.53		18660617	L	0.000000E0
	38004.20000	27.70		38004500	L	0.000000E0
	2617.59000	29.10		2617603	F	0.000000E0
	713326.00000	30.06		713334737	EF	0.000000E0
	567469.00000	31.86		567476108	EF	0.000000E0

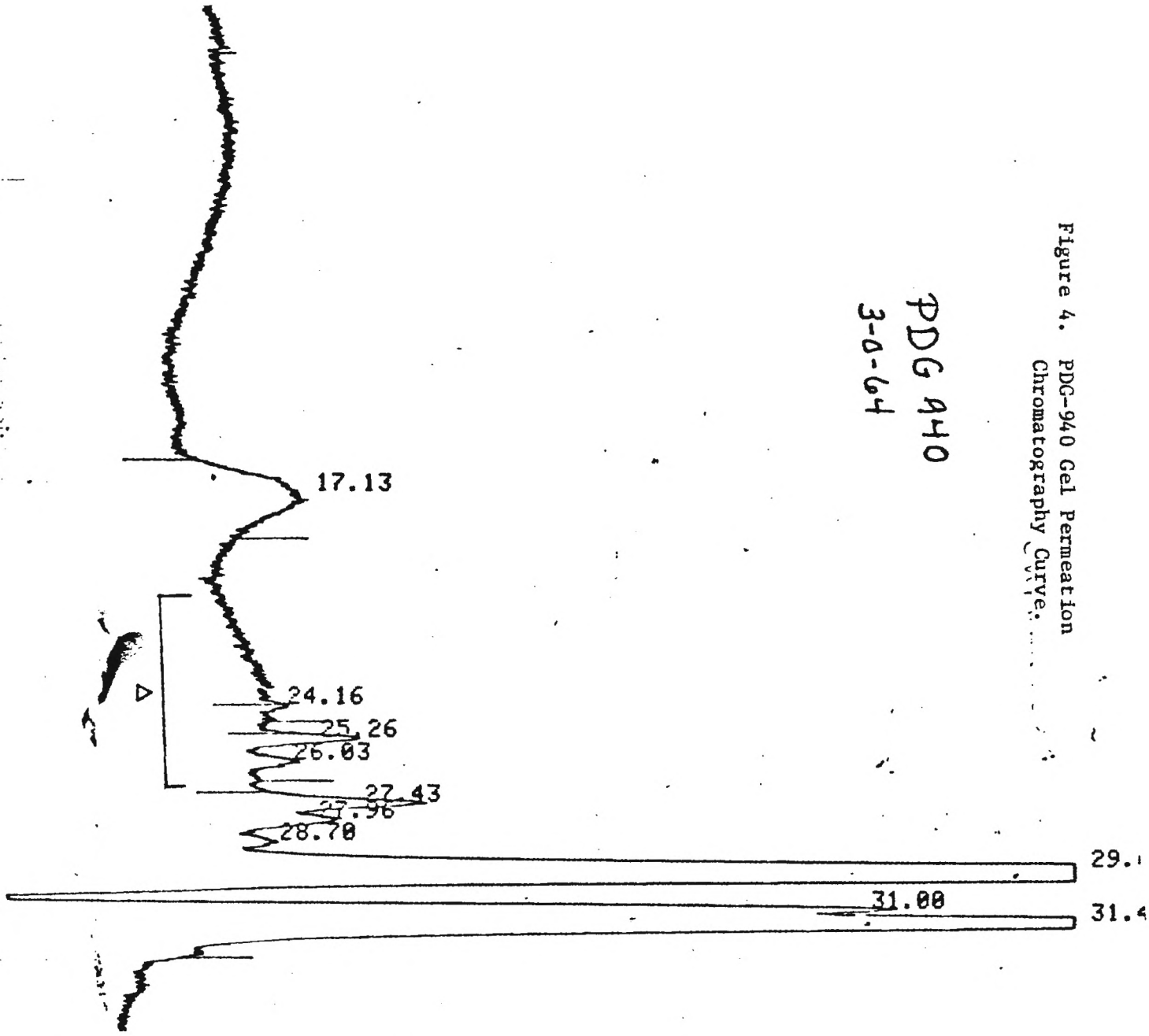

PDG 940
3-0-64

Figure 4. PDG-940 Gel Permeation Chromatography Curve.

AUG. 25, 1983 06:16:18 CHART 0.50 CM/MIN
RUN #54 CALC #0
COLUMN SOLVENT OPR ID: 6

EXTERNAL STANDARD QUANTITATION

PEAK#	AMOUNT	RT	EXP RT	AREA		RF
	**********	17.13		1157666124	L	0.000000E0
	216859.00000	24.16		216861765	L	0.000000E0
	232605.00000	25.26		232606976	F	0.000000E0
	433093.00000	26.03		433098211	L	0.000000E0
	257336.00000	27.43		257338807	F	0.000000E0
	238970.00000	27.96		238973208	F	0.000000E0
	9060.44000	28.70		9060485	F	0.000000E0
	**********	29.63		1122320171	EF	0.000000E0

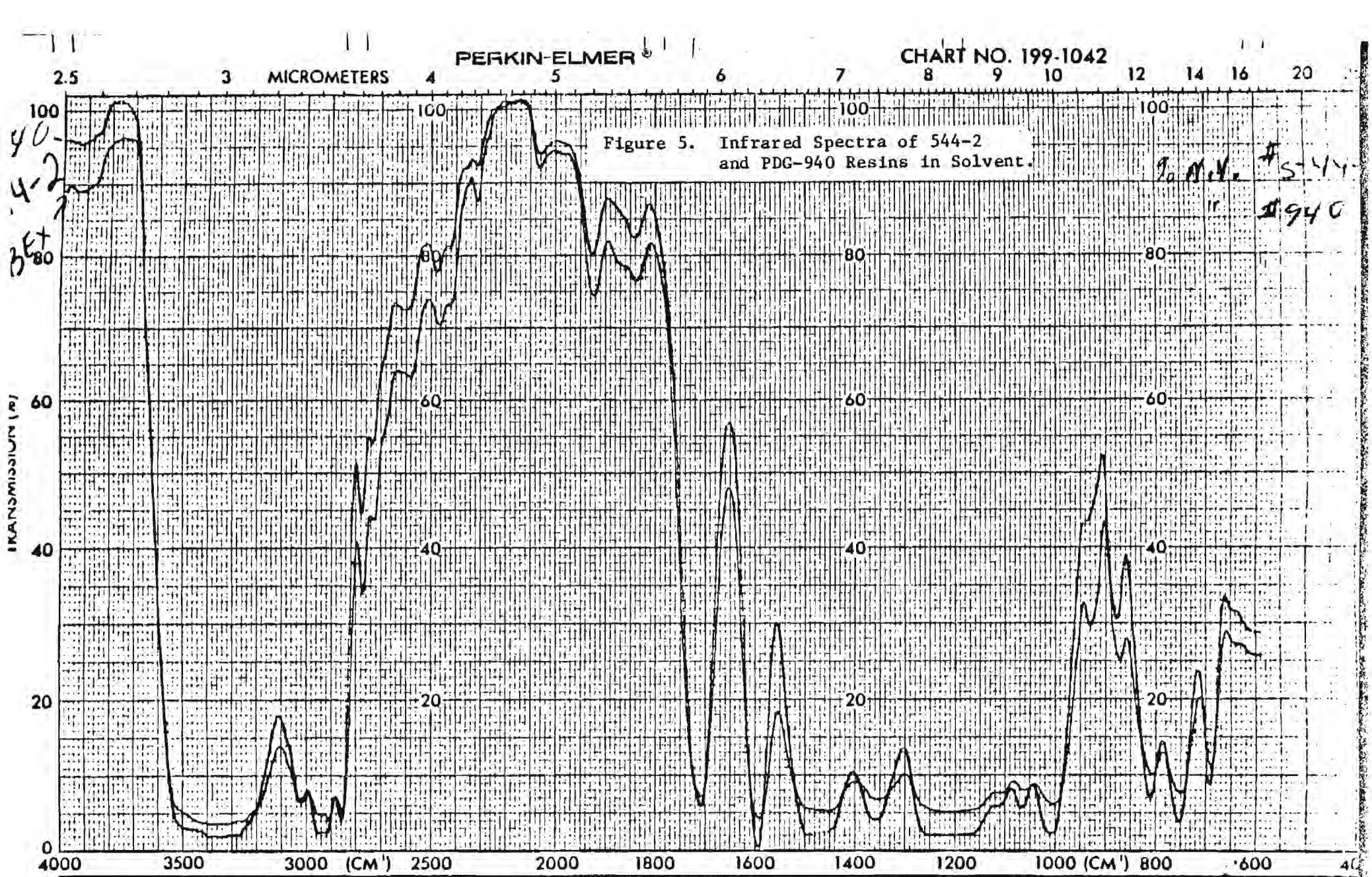
PERKIN-ELMER
CHART NO. 199-1042
2.5
3
MICROMETERS
4
5
6
7
8
9
10
12
14
16
20
100
80
60
40
20
0
TRANSMISSION (%)
4000
3500
3000 (CM')
2500
2000
1800
1600
1400
1200
1000 (CM')
800
600
40
Figure 5. Infrared Spectra of 544-2 and PDG-940 Resins in Solvent.
ABSCISSA
EXPANSION
ORDINATE
EXPANSION
% T
ABS
SCAN TIME
MULTIPLIER
SLIT PROGRAM
REP. SCAN
SINGLE BEAM
TIME DRIVE
OPERATOR
DAT
SAMPLE
ORIGIN
REMARKS
SOLVENT
CONCENTRATION
CELL PATH
REFERENCE

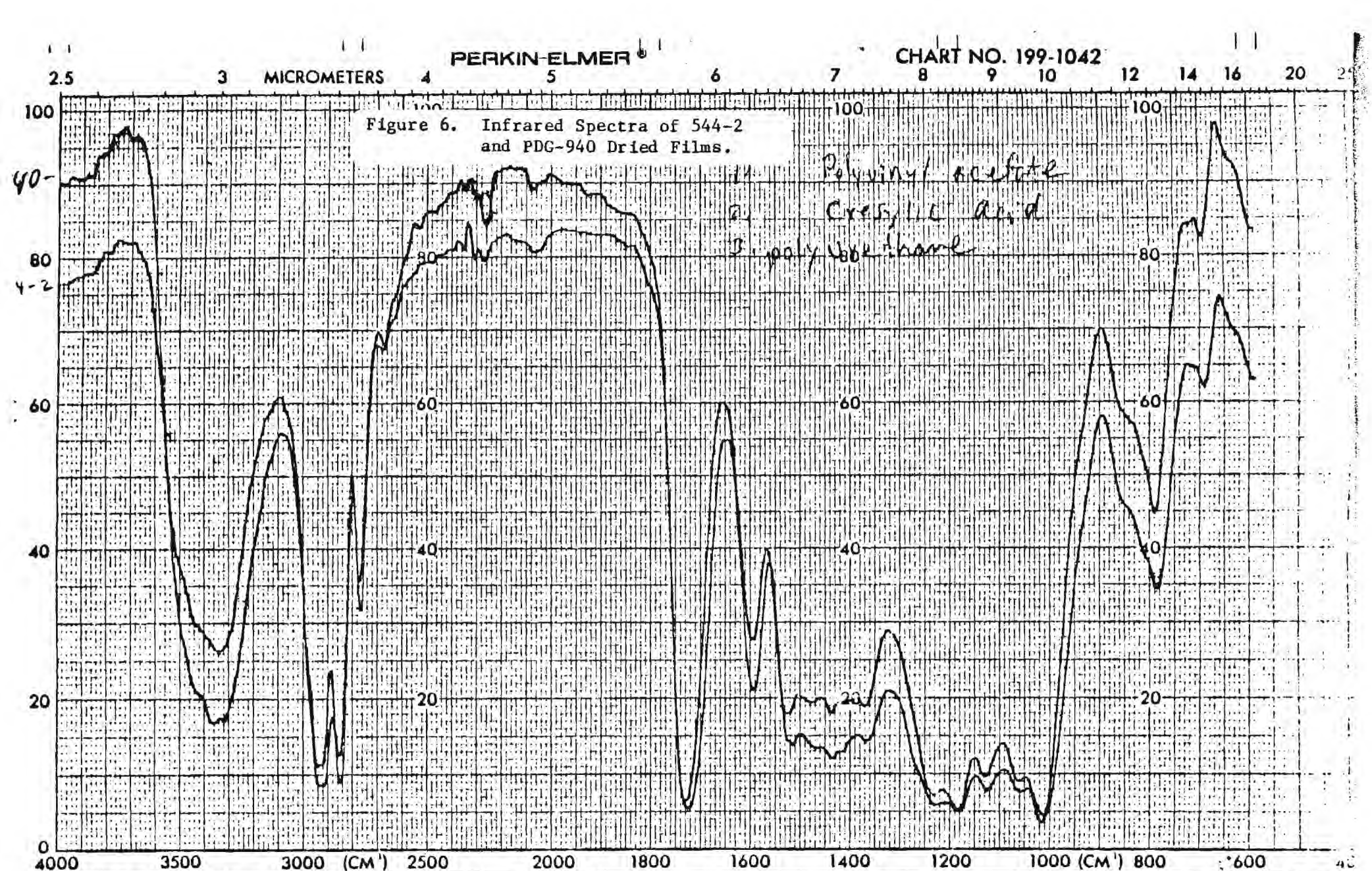

ABSCISSA	ORDINATE	SCAN TIME	REP. SCAN / SINGLE BEAM
EXPANSION	EXPANSION	MULTIPLIER	TIME DRIVE
	% T / ABS	SLIT PROGRAM	OPERATOR / DATE

SAMPLE / ORIGIN	REMARKS	SOLVENT / CONCENTRATION	CELL PATH / REFERENCE
SAMPLE fuselage house ORIGIN Dry			